



## MODELLING OF SURFACE ROUGHNESS AND MATERIAL REMOVAL RATE IN LASER BEAM MACHINING OF $Al_2O_3/CNT$ USING TAGUCHI TECHNIQUE

Yemmani Suresh Babu<sup>1\*</sup>, Syed Altaf Hussain<sup>2</sup>, B.Durga Prasad<sup>3</sup>

<sup>1</sup>Ph.D. Research Scholar, Mechanical Department, Jawaharlal Nehru Technological University Anantapur, Ananthapuramu, Andhra Pradesh-515002, India, Email: - yemmanisuresh@gmail.com

<sup>2</sup>Professor, Mechanical Department, Rajeev Gandhi Memorial College of Engineering and Technology, Nandyal, Andhra Pradesh,-518501, India.

<sup>3</sup>Professor, Mechanical Department, Jawaharlal Nehru Technological University Anantapur, Ananthapuramu, Andhra Pradesh, India.

**\*Corresponding Author:** - Yemmani Suresh Babu

<sup>\*</sup>Ph.D. Research Scholar, Mechanical Department, Jawaharlal Nehru Technological University Anantapur, Ananthapuramu, Andhra Pradesh-515002, India, Email: - yemmanisuresh@gmail.com

---

### Abstract:-

Laser machining stands as a leading noncontact method in advanced manufacturing. Its prowess lies in crafting intricate surfaces, structures, and electro-mechanical devices, often on a minute scale, using laser energy. Unlike traditional methods, this process relies on the thermophysical characteristics of materials rather than their mechanical traits. Crafting an optimal surface quality and material removal depends heavily on fine-tuning process parameters.

In a recent study, laser beam machining using a nanosecond pulse ytterbium fiber laser on alumina ceramic was investigated. The focus was on understanding the impact of cutting speed, oxygen pressure, and the percentage of carbon nano tubes (CNT) in the alumina matrix on material removal efficiency and surface finish quality. This exploration delved into the development of  $Al_2O_3/CNT$  composites, analyzing variations in the weight percentages of carbon nano tube materials within the alumina structure.

**Keywords:** - $Al_2O_3/CNT$ ; Laser beam machining; Taguchi; material removal rate; surface roughness

### 1. Introduction

Numerous ceramic materials, including alumina ( $Al_2O_3$ ), zirconia ( $ZrO_2$ ), magnesia ( $MgO$ ), silicon carbide ( $SiC$ ), and silicon nitride ( $Si_3N_4$ ), find extensive applications across a diverse range of industries. These sectors encompass microelectronics, automotive, aerospace, printing, textile, medical, and biotechnological domains. The widespread adoption of these ceramics is primarily due to their exceptional characteristics, which include the ability to maintain structural integrity under high temperatures, outstanding resistance to wear and thermal shocks, chemical inertness, superior electrical properties, and a lower density [1, 2]. The distinctive mechanical and physical characteristics of structural ceramics present considerable challenges when attempting to fashion them into desired components through conventional machining techniques. The obstacles hindering the production of precise ceramic components via traditional machining methods include issues

such as unacceptable tool wear, inadequate precision, and potential mechanical or thermal damage to the workpiece [3 – 5].

Laser beam machining emerges as a promising and cutting-edge solution for the efficient removal of bulk material and the creation of intricate ceramic components. Extensive experimental and numerical studies have been conducted using different laser types and operational modes to determine the most effective process parameters for achieving both successful material removal and exceptional surface quality in the machined components. Numerous researchers have directed their efforts towards investigating laser drilling [6 – 9] and laser cutting [10 – 12] of alumina ceramics. Their studies have shed light on the impact of various laser machining parameters on factors such as material removal rates and the quality of the machined surfaces, which encompasses considerations like surface finish, the extent of the heat-affected zone, debris generation, and the formation of thermal cracks. Research has been conducted to explore the intricate laser-material interactions and the underlying physical phenomena that occur during one-, two-, and three-dimensional laser machining of alumina ceramics. Additionally, the impact of both stationary and moving laser beams on the resultant surface finish has been carefully assessed in these studies [13 – 17]. As per the findings from these studies, it was observed that surface roughness exhibited an upward trend as the average laser energy density, pulse rate, and lateral distance (laser beam overlap) increased. Furthermore, the rise in crater depth and the accumulation of material around the machined cavity were predominantly attributed to material loss through evaporation and the fluid flow induced by recoil pressure [16]. Utilizing a combination of short-pulse lasers with shorter wavelengths typically yields superior outcomes in ceramic laser machining. However, it's important to note that thermal stresses generated during the machining process can lead to cracking. Therefore, it becomes essential to establish optimized process parameters that minimize heat input into the bulk material, thereby preventing the formation of cracks. Micromachining employing longer pulse lasers, operating in the micro- and millisecond time regimes, involves a material removal mechanism that incorporates melting.

While this method holds the potential for achieving remarkably high material removal rates, it also tends to generate a glassy layer, which is frequently regarded as the origin of micro-cracks [3, 4].

The introductory statement suggests that extensive analysis of the existing literature highlights a particular challenge within the field of laser machining. While numerous studies have been dedicated to enhancing laser machining parameters for improved material removal efficiency and the quality of machined surfaces, achieving the desired surface finish in pulse-mode laser beam machining remains a notable and unresolved issue. In other words, despite significant research efforts, this aspect continues to pose challenges, indicating that there is a gap in our understanding and a need for further investigation.

Recognizing this gap, the paper's objective is clearly outlined. The study aims to experimentally investigate how various laser beam parameters influence the surface morphology of machined components. To conduct this investigation, the researchers utilize a nanosecond pulse fiber laser and select alumina ceramics as the working material. This choice of material and laser type underscores the study's specific focus on addressing the challenges associated with achieving the desired surface finish in laser machining, particularly in the context of pulse-mode laser beam technology. By conducting this experimental study, the research aims to contribute to the body of knowledge in this area and potentially provide insights that can lead to improvements in the precision and quality of laser machining processes for ceramics.

## **2. Design of experiments (DOEs)**

### **2.1 Taguchi design methodology**

The objective of the Taguchi design is to determine the optimum level of input process parameters that makes the process insensitive against the effects of variations due to uncontrollable factors or noise factors such as environmental temperature, humidity and vibration. To accomplish this objective, Taguchi has designed experiments using especially constructed tables known as

‘orthogonal array’ (OA). The use of these tables makes the DOEs very easy and consistent. The selection of OA is based on the total degree of freedom (DOF) of the process which is calculated as Phadke [18] and Ross [19].

In present case four input parameters are selected each at three levels and no interaction has been assumed between them. Therefore, the total DOF is found as:  $DOF = (3 - 1) \times 4 + 1 = 9$ .

In general, signal to noise (S/N) ratio ( $\eta$  dB) represents the quality characteristics for the observed data in the Taguchi DOEs. Here, signal represents the desirable value and noise represents the undesirable value. The S/N ratio expresses the scatter around the desired value and larger S/N ratio will give the smaller scatter. Depending upon the experimental objectives, there may be several quality characteristics. Mathematically, the S/N ratio for quality characteristics can be computed as Phadke [18] and Ross [19].

$$\eta = -10 \log_{10}(MSD) \quad (1)$$

Where, MSD = mean square deviation from the desired value and commonly known as quality loss function. The MSD is different for different type of characteristics.

In the present case of average kerf taper (Ta) and average surface roughness (Ra), smaller values of them are desirable. These quality loss functions in the Taguchi method termed as the smaller-the-better (SB) type characteristics and are defined as follows:

$$MSD = \left( \frac{1}{n} \sum_{j=1}^n y_j^2 \right) \quad (2)$$

Where,  $y_j$  are the observed data (or quality characteristic) of the  $j^{\text{th}}$  trial and  $n$  is the number of replications at the same condition of experiment.

In the process with multiple quality characteristics, the optimal search for input process parameters is called as multi-objective optimisation problem where a single overall S/N ratio for all quality characteristics is computed in stead of separate S/N ratio for each quality characteristic. This overall S/N ratio is known as multiple S/N ratio (MSNR). Before calculating the MSNR, it is important to normalise the quality loss of each quality characteristic because each has different units of measurement [20]. The normalised quality loss (NQL) can be computed using:

$$y_{ij} = \frac{L_{ij}}{L_j^*} \quad (3)$$

Where,  $y_{ij}$  is the NQL associated with the  $i^{\text{th}}$  quality characteristic at  $j^{\text{th}}$  experimental run and it varies from a minimum of zero to maximum of one.  $L_{ij}$  is the quality loss for the  $i^{\text{th}}$  quality characteristic at the  $j^{\text{th}}$  run, and  $L_j^{**}$  is the maximum quality loss for  $i^{\text{th}}$  quality characteristic among all the experimental runs.

For computing the TNQL ( $Y_j$ ) corresponding to each run, we must assign a weighting factor for each quality characteristic considered in the optimisation process [20]. If  $w_i$  represents the weighting factor for the  $i^{\text{th}}$  quality characteristic,  $p$  is the number of quality characteristics then  $Y_j$  can be computed using:

$$Y_j = \sum_{i=1}^p W_i y_{ij} \quad (4)$$

After finding the TNQL, the next step is to compute the MSNR ( $\eta_j$ ) at each experimental condition. This is given as:

$$Y_j = -10 \log_{10} (Y_j) \quad (5)$$

## 2.2 Response Surface Methodology

RSM is a collection of mathematical and statistical techniques that are useful for the modelling and analysis of problems in which a response of interest is influenced by several variables and the main objective is to optimise this response. The necessary data for building the response models and optimisation of manufacturing processes are collected by the DOEs. RSM also quantifies the relationship between the input process parameters and the obtained responses. The quantitative form of relationship between desired response and independent input variables could be represented as:

$$Y = f(x_1, x_2, x_3, \dots, x_n) + \varepsilon \quad (6)$$

Where  $y$  is the desired response,  $f$  the response function (response surface  $(x_1, x_2, x_3, \dots, x_n)$  are the independent input variables, and  $\varepsilon$  is the fitting error.

In order to study the effects of laser cutting parameters a second order polynomial response surface mathematical model has been considered as follows:

$$\hat{Y} = \beta_0 + \sum_{i=1}^K \beta_i X_i + \sum_{i=1}^K \beta_{ii} X_i^2 + \sum_i \sum_j \beta_{ij} X_j + \varepsilon \quad (7)$$

Where all  $b$ 's are regression coefficients determined by least square method [21]. To estimate the regression coefficients in this model, each variable  $x_i$  must take at least three different levels. This suggests the use of FD of the 3<sup>p</sup> series but it is a tedious work with large number of factors. For fitting second order model a new design known as CCD is generally used [22]. There are two parameters in the design that must be specified: the distance  $\alpha$  of the axial runs from the design centre and the number of centre points. The value of  $\alpha$  must be  $(2)^{p/4}$  in order to make the design rotatable.

It is important for the second order model to provide good predictions throughout the region of interest. So the model should have a reasonably consistent and stable prediction of responses at points of interest  $x_i$ . This can be achieved by CCRD. In CCRD, the standard error is the same for all points that are at the same distance from the centre of the region. Mathematically, this can be stated as [22].

$$x^2_1 + x^2_2 + x^2_3 + \dots + x^2_p = Constant \quad (8)$$

CCRD requires minimum five levels of all input parameters for the calculation of regression coefficients. In this situation, the total number of runs required becomes  $2p + 2^*p +$  more than one runs at centre [22].

## 3. Experimental Details

In this study, the influence of laser beam machining parameters on the machined surface morphology was experimentally studied applying the nanosecond pulse ytterbium fibre laser and Al<sub>2</sub>O<sub>3</sub>/CNT as working material. The influence of Oxygen Pressure, Pulse frequency /Repetition Rate, Cutting speed, Wt.% of CNT on surface finish and material removal rate and the quality of machined surface was examined via Taguchi method (L27 orthogonal matrix was used) in the preliminary experiment [23]. The aim of preliminary experiment was to define the laser beam machining parameters which affect the machined surface quality in significant way. These chosen parameters and its levels are summarized in Tab. 1, but a number of experiments required by a 3k full factorial design having four factors is 81. Therefore the Taguchi orthogonal matrix L25 was chosen for the experiment realization, 25 runs have been carried out.

**Table 1.** Process parameters and levels used for the experimentation

Symbol/ Variable	Process Parameters	Units	Levels				
			1	2	3	4	5
P <sub>1</sub>	Oxygen Pressure	Kg/cm <sup>2</sup>	2	3	4	5	6
P <sub>2</sub>	Pulse frequency / Repetition Rate	Hz	5	10	15	20	25
P <sub>3</sub>	Cutting speed	mm/min	10	20	30	40	50
P <sub>4</sub>	Wt.% of CNT	%	1	3	5	7	9

The experiment has been performed using a high precision laser machining centre Mogad Laser Machining Pvt. Ltd., Bangaloure, 80 Shape equipped by solid-state pulsed fiber ytterbium laser with an average output power of 100 W, pulse duration of 120 ns and wavelength of 1064 nm as shown in Figure 2.

Al<sub>2</sub>O<sub>3</sub>/CNT with various percentages of (1%, 3%, 5%, 7% and 9%) was chosen as the working material (manufacturer Glynwed, GmbH). It is an easily producible and relatively cheap type of ceramic with the following properties:

apparent density of 3.7 – 3.95 g.cm<sup>-3</sup>, mean grain size of 10 μm, hardness (Knopp, 100 g) of 23000 MPa, specific heat of 850 J.kg<sup>-1</sup>.K<sup>-1</sup> and thermal conductivity of 30 W.m<sup>-1</sup>.K<sup>-1</sup>. Testing samples were a cylindrical and square in shape with the diameter of 10 mm and the thickness of 3 mm. Testing cavities (squared in shape with a side length of 2.5 mm) have been manufactured on the planar surfaces of testing sample (average surface roughness Ra of 3.56 μm) at a given combination of laser beam parameters. The shape and the dimensions of the testing sample and the testing cavities arrangement are depicted on the Fig. 1.

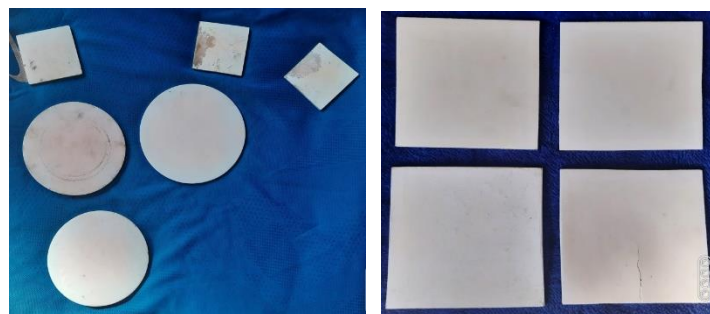


**Figure 1.** planar surface of the testing sample

Experimental results revealed that the laser pulse energy (defined by the Oxygen Pressure, Pulse frequency /Repetition Rate,) and Wt.% of CNT affect the studied surface roughness and material removal rate and quality of machined surface significantly. Material ablation has taken part in laser micro-machining process only if the pulse frequency values are higher than 25Hz. Machined surface quality is affected by the Oxygen Pressure, Pulse frequency /Repetition Rate, Cutting speed, Wt.% of CNT significantly. This preliminary experiment confirmed difficult machinability of Al<sub>2</sub>O<sub>3</sub>/CNT of various percentages of CNT i.e., 1%, 3%, 5%, 7% and 9% and defined main process parameters: Oxygen Pressure, Pulse frequency /Repetition Rate, which will be analyzed subsequently in more detailed way described in the next part of the paper.

**Table 2.** Design Matrix with coded & uncoded values

Exp No.	Coded Values				Original Values			
	Oxygen Pressure (Kg/cm <sup>2</sup> )	Pulse frequency (Hz)	Cutting speed (mm/ min)	Wt. % of CNT (%)	Oxygen Pressure (Kg/cm <sup>2</sup> )	Pulse frequency (Hz)	Cutting speed (mm/min)	Wt.% of CNT (%)
1	1	1	1	1	2	5	10	1
2	1	2	2	2	2	10	20	3
3	1	3	3	3	2	15	30	5

4	1	4	4	4	2	20	40	7
5	1	5	5	5	2	25	50	9
6	2	1	2	3	3	5	20	5
7	2	2	3	4	3	10	30	7
8	2	3	4	5	3	15	40	9
9	2	4	5	1	3	20	50	1
10	2	5	1	2	3	25	10	3
11	3	1	3	5	4	5	30	9
12	3	2	4	1	4	10	40	1
13	3	3	5	2	4	15	50	3
14	3	4	1	3	4	20	10	5
15	3	5	2	4	4	25	10	7
16	4	1	4	2	5	5	40	3
17	4	2	5	3	5	10	50	5
18	4	3	1	4	5	15	10	7
19	4	4	2	5	5	20	20	9
20	4	5	3	1	5	25	30	1
21	5	1	5	4	6	5	50	7
22	5	2	1	5	6	10	10	9
23	5	3	2	1	6	15	20	1
24	5	4	3	2	6	20	30	3
25	5	5	4	3	6	25	40	5

In machining process identifying the low surface finish and maximum material removal rate in Al<sub>2</sub>O<sub>3</sub>/CNT composites. Table 1 shows the experimental conditions used machining process. Figure 2 demonstrates the experimental setup used for machining of Al<sub>2</sub>O<sub>3</sub>/CNT.



**Figure 2.** Laser Machining Process

#### 4. Results and Discussion

In this experiment, laser beam power as an input factor was chosen with the 25 levels. Oxygen Pressure, Pulse frequency /Repetition Rate, cutting speed and Wt.% of CNT input parameters. Table. 1 summarizes the chosen parameters and its levels for this experimental analysis.

The testing cavities squared in shape with the side length of 3 mm are produced. The depth of testing cavities varies, depending on the pulse frequency. The material removal rate was determined as the ratio of the removed material volume and the machining time.

The obtained surface finish and MRR values are summarized in Table. 3. It can be seen, that the surface finish as well as the MRR values rise with the increasing values of pulse frequency, while the functionality between the oxygen pressure, cutting speed and wt.% of CNT and the MRR is highly linear.

**Table 3.** Experimental conditions and results.

S.No.	Oxygen Pressure (Kg/cm <sup>2</sup> )	Pulse frequency (Hz)	Cutting speed (mm/min)	Wt.% of CNT (%)	Surface Roughness (Ra)	Material Removal Rate (MRR)
1.	4	5	10	1	3.56	1.28
2.	4	10	20	3	4.32	1.51
3.	4	15	30	5	5.46	1.52
4.	4	20	40	7	5.58	1.65
5.	4	25	50	9	6.15	1.86
6.	6	5	20	5	4.56	1.35
7.	6	10	30	7	4.35	1.62
8.	6	15	40	9	5.53	1.56
9.	6	20	50	1	3.86	1.98
10.	6	25	10	3	6.32	1.42
11.	8	5	30	9	4.96	1.65
12.	8	10	40	1	3.67	1.93
13.	8	15	50	3	3.98	1.90
14.	8	20	10	5	5.12	1.56
15.	8	25	10	7	5.24	1.56
16.	9	5	40	3	3.97	1.96
17.	9	10	50	5	4.07	1.72
18.	9	15	10	7	4.47	1.46
19.	9	20	20	9	5.45	1.56
20.	9	25	30	1	4.19	2.21
21.	10	5	50	7	4.23	1.86
22.	10	10	10	9	4.32	1.35
23.	10	15	20	1	4.34	2.50
24.	10	20	30	3	4.36	2.23
25.	10	25	40	5	4.52	2.12

#### 4.1 Mathematical model for machining responses

The second order response surface model representing the surface roughness & material removal rate can be communicated as function of cutting parameters are Oxygen Pressure, Pulse frequency /Repetition Rate, cutting speed and Wt.% of CNT The test esteems are examined using response surface analysis and the accompanying relation has been established for surface finish and material removal rate in uncoded units.

All RSM issues utilize either of these models. The  $\beta$  coefficients, used as a part of the above model can be ascertained by means for using the minimum squares strategy. The second-order show is typically used when the response function isn't known or nonlinear. In the present examination a second order show has been used. The test values are analyzed and the accompanying relation is acquired for wear. The machining responses in uncoded values is given by:

$$\text{Ra} = -0.55 + 1.031 P_1 + 0.374 P_2 - 0.023 P_3 - 0.178 P_4 - 0.0597 P_1^2 - 0.00218 P_2^2 - 0.001909 P_3^2 - 0.0127 P_4^2 + 0.0391 P_1 * P_2 + 0.0082 P_1 * P_3 + 0.0237 P_1 * P_4 + 0.00158 P_2 * P_3 + 0.00342 P_1 * P_4 + 0.00630 P_3 * P_4 \quad (10)$$

$$\text{MRR} = 0.572 + 0.056 P_1 - 0.0678 P_2 + 0.1184 P_3 - 0.271 P_4 + 0.0110 P_1^2 + 0.001208 P_2^2 - 0.000369 P_3^2 - 0.00333 P_4^2 + 0.00899 P_1 * P_2 - 0.01123 P_1 * P_3 + 0.0139 P_1 * P_4 - 0.001196 P_2 * P_3 - 0.00029 P_2 * P_4 + 0.00426 P_3 * P_4 \quad (11)$$

The ampleness of the developed model can be verified by using R<sup>2</sup> value after estimating sum of squares (SS) and mean squares (MS). The amount R<sup>2</sup>, called coefficient of assurance, is used to judge the ampleness of regression model created, 0 ≤ R<sup>2</sup> ≤ 1. The R<sup>2</sup> values is the variability in the information represented by the model in percentage [24,25].

$$R^2 = 1 - \frac{SS\ Error}{SS\ Total} \quad (12)$$

The coefficient of assurance is calculated for wear using the above articulation and is 97.92%, which demonstrates the high correlation that exists between the test and anticipated esteems. Table 7 shows the analysis of variance carried out for surface roughness and material removal rate. The F-values in the table demonstrates that the developed model is very satisfactory at 95% confidence level. Further, the near outcomes between the test esteems and the response surface model values are displayed in Figure 4. Additionally, the variations between the experimental results and model predicted values are analyzed through residual graphs, and are exhibited in Figure 3 and Figure 4. Residual is the variation between the experimental esteems and model values. From the examination of the residual charts, it has been discovered that there is no abnormal variation between the experimental values and predicted esteems, and thus the created model is highly significant and can be used for the prediction of wear in MMC.

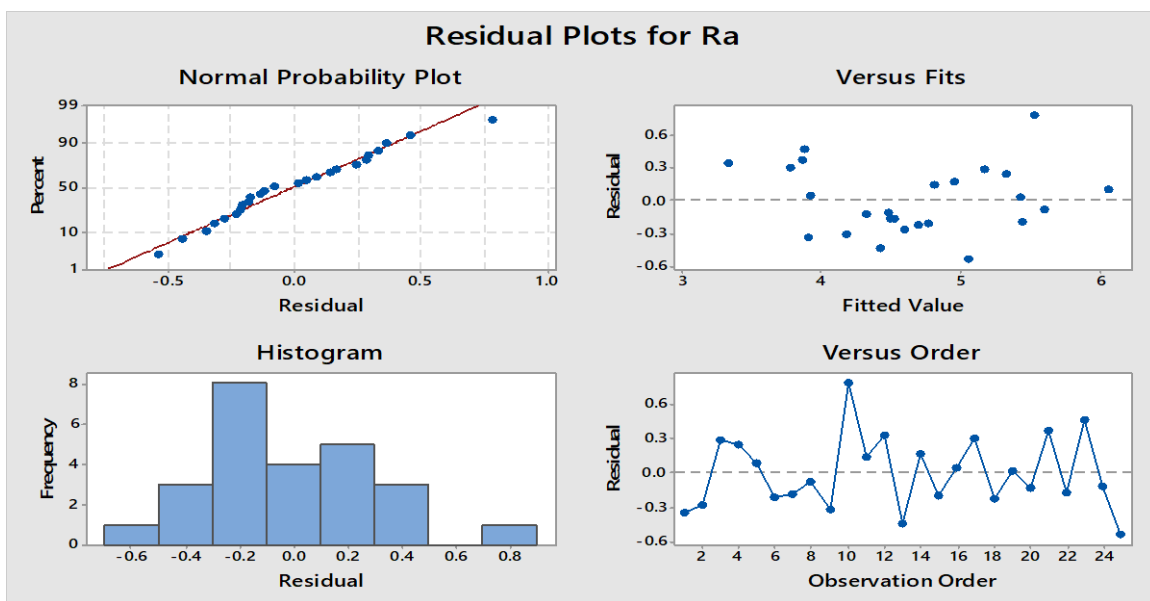


Figure 3. Residual analysis for average experimental values with respect to predicted values.

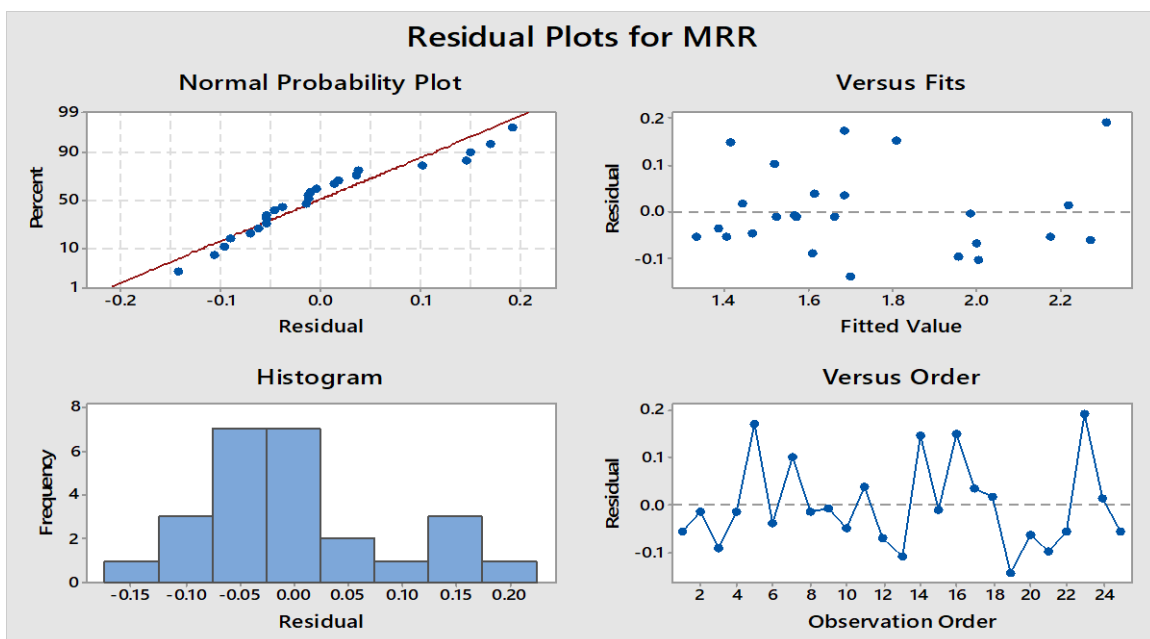


Figure 4. Residual analysis for average experimental values with respect to predicted values.



**Table 4.** Analysis of Variance for surface roughness

Source	DF	Adj SS	Adj MS	F-Value	P-Value
Oxygen Pressure	4	1.7127	0.42818	1.44	0.305
Pulse frequency	4	4.3267	1.08167	3.65	0.056
Cutting speed	4	0.3582	0.08955	0.30	0.869
Wt.% of CNT	4	4.7926	1.19816	4.04	0.044
Error	8	2.3734	0.29668		
Total	24	13.5887			

Result of ANOVA for the response function surface finish and roughness is introduced in Table 4 and Table 5. This examination is done for a level of significance of 5% i.e., for a level of confidence of 95%. From the investigation if Table 4, it is clear that, the F calculated esteems is more prominent than the F-table esteems (F 0.05, 14,16 = 2.37) and hence the second order response function developed is quite is very satisfactory [19,20 and 24].

**Table 5.** Analysis of Variance for material removal rate

Source	DF	Adj SS	Adj MS	F-Value	P-Value
Oxygen Pressure	4	0.6632	0.16580	6.79	0.011
Pulse frequency	4	0.2877	0.07192	2.94	0.091
Cutting speed	4	0.7729	0.19323	7.91	0.007
Wt.% of CNT	4	0.4543	0.11358	4.65	0.031
Error	8	0.1955	0.02444		
Total	24	2.3367			

**5. Effect of Oxygen Pressure, Pulse frequency /Repetition Rate, cutting speed and Wt.% of CNT**

**5.1 Analysis of Surface Roughness**

The trend of surface roughness and material removal rate with respect to cutting speed is shown in Figure 5 (a-c).

The plots are drawn using response surface model for surface roughness and material removal rate using laser beam machining process. The plots are drawn between the surface roughness and cutting speed by keeping Oxygen Pressure, Pulse frequency /Repetition Rate, as constant at mid level for Al<sub>2</sub>O<sub>3</sub> /CNT, whose wt.% of CNT varied from 1% to 9%.

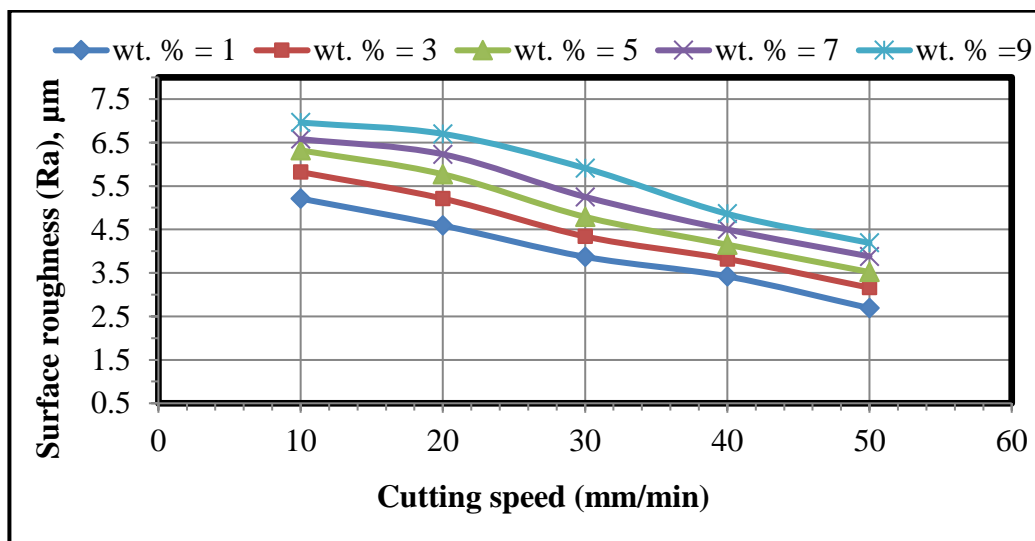


**Figure 5 (a).** Effect of wt.% of CNT on surface roughness with varying Cutting speed

The effects of cutting speed on Ra are shown in Figure 5(a). Oxygen pressure and plus frequency are taken as constant. From the graph it has been observed that Ra decreases with increasing cutting speed when cutting speed is kept at higher level.s At higher level of cutting speed, Ra increases with the increase of wt.% of CNT because at higher cutting speed the process becomes faster and in addition to that due to increased beam overlapping rate the laser interacts rapidly with the composite material for the constant oxygen pressure and plus frequency. Finally, as the cooling time available to resolidify the molten composite material get reduces and thus producing low Ra value [5,6].

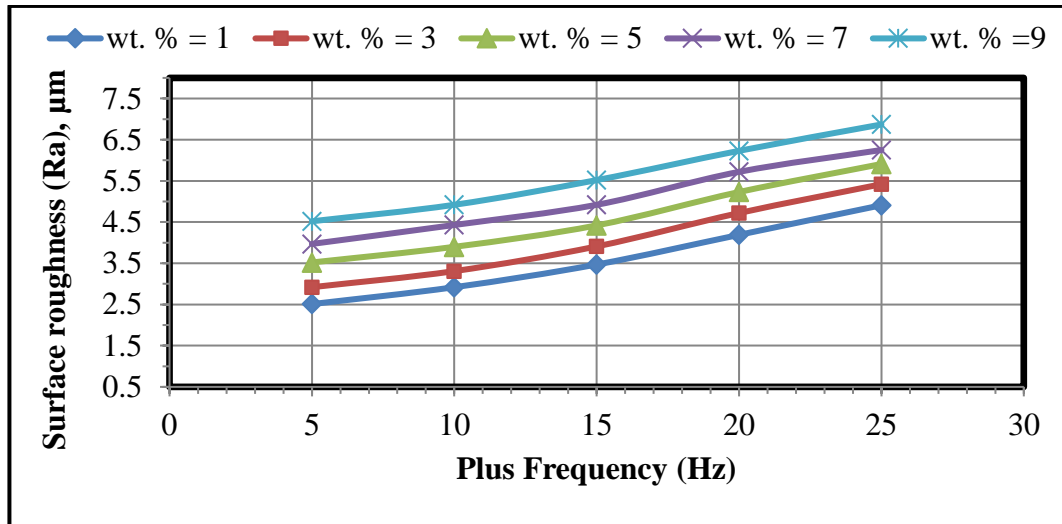


Figure 5 (b). Effect of wt.% of CNT on surface roughness with varying plus frequency

Figure 5 (b) exhibits the effects of pulse frequency on Ra by keeping the oxygen pressure and cutting speed constant. From the response graph, it has been observed that Ra first increases following a parabolic curve with change in oxygen pressure and cutting speed. But with the increase of pulse frequency, Ra first decreases slightly then increases gradually at last for different values of plus frequency. At higher pulse frequency, laser rapidly interacts with the work sample of Al<sub>2</sub>O<sub>3</sub>/CNT causing cooling time to be reduced and thus reducing the chances of resolidification of the molten material, resulting in good surface finish or lower Ra. Surface plot shows the same variation in Ra with the increase of pulse frequency for different value of oxygen pressure and cutting speed.

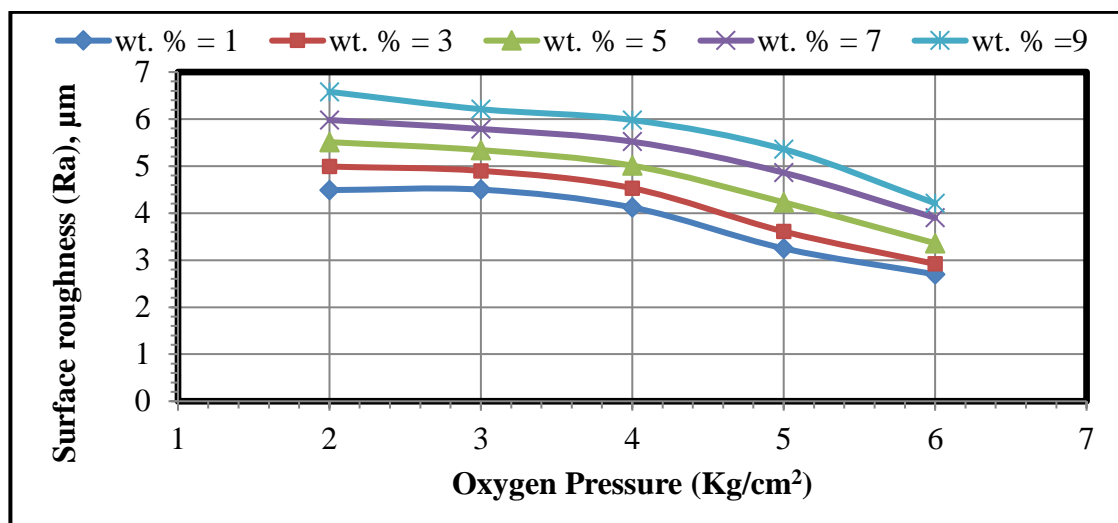


Figure 5 (c). Effect of wt.% of CNT on surface roughness with varying Oxygen

From the Figure 5(c) of Ra, the effects of oxygen pressure at constant plus frequency, cutting speed can be analysed. It has been observed that Ra decreases with the increase of oxygen pressure for higher value of oxygen pressure. Because higher oxygen pressure means more interaction time between laser and work samples of Al<sub>2</sub>O<sub>3</sub> /CNT's and increased oxygen pressure gives higher beam overlapping rate which allows sufficient energy to melt the composite material for quality cutting. Keeping oxygen pressure at higher value, results in good surface finish Ra whereas the increments of oxygen pressure increases Ra at the initial stage and later on it decreases following a parabolic curve at higher level of pressure.

### 5.2 Analysis of Material Removal Rate

The trend of material removal rate with respect to cutting speed for the laser beam machining process are shown in Figure 6 (a-c).

The graphs are drawn using response surface model for material removal rate using laser beam machining process. The plots are drawn between the material removal rate and cutting speed by keeping oxygen pressure, plus frequency as constant at mid level for machining of Al<sub>2</sub>O<sub>3</sub> / CNT, for different wt.% of CNT, whose CNT content is vary from 1% to 9% in the matrix material.

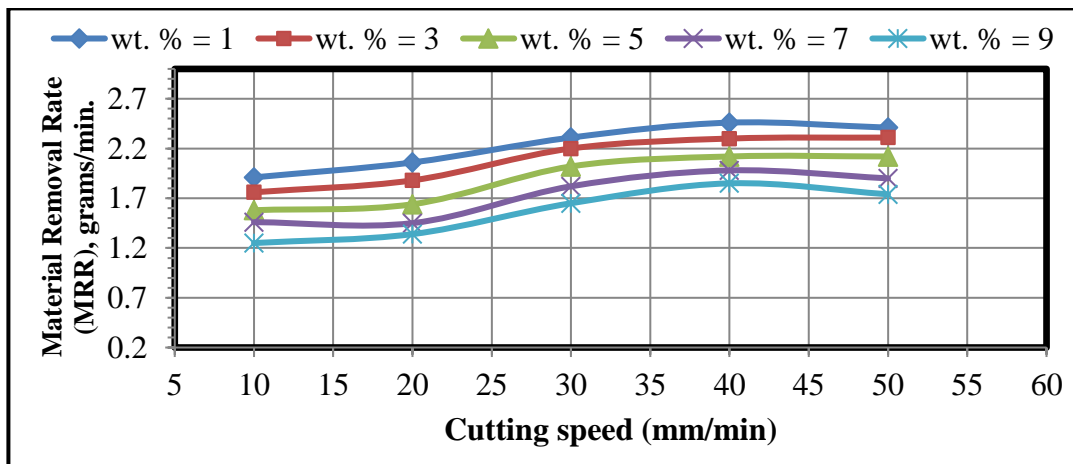


Figure 6 (a). Effect of wt.% of CNT on surface roughness with varying Cutting speed

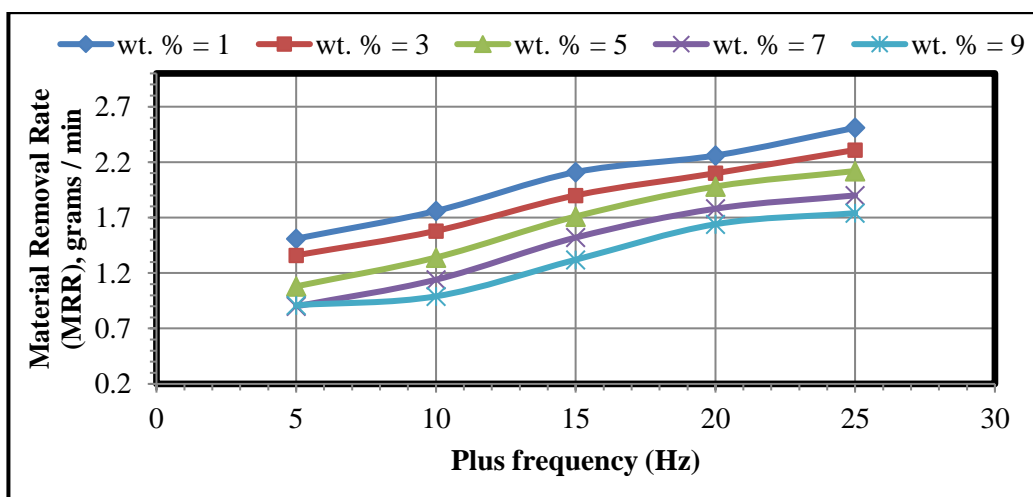


Figure 6 (b). Effect of wt.% of CNT on surface roughness with varying Plus frequency

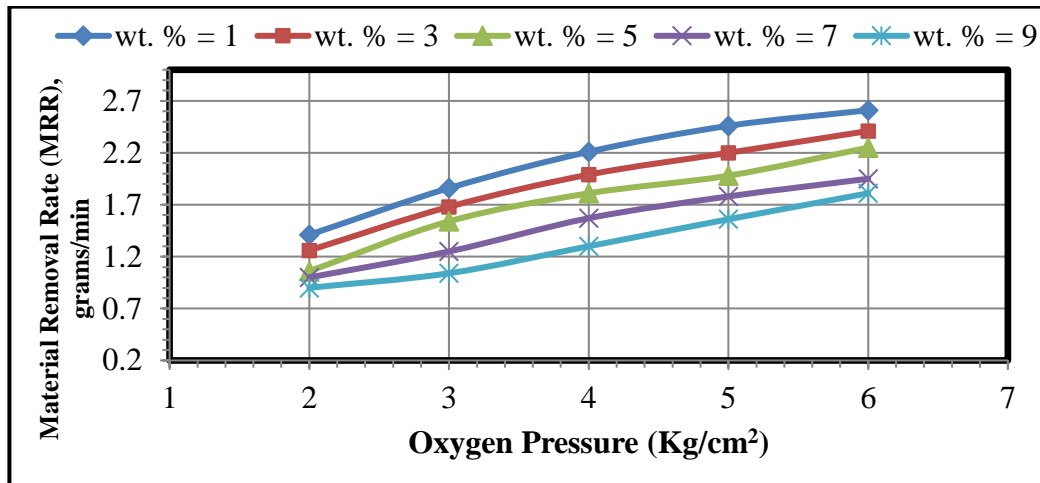


Figure 6 (c). Effect of wt.% of CNT on surface roughness with varying Oxygen Pressure

From figure 6 it is inferred that high material removal rate are observed with increases of plus frequency as compare to low plus frequency. Because of CNT particles are equally spread in alumina matrix material. Figure 6 shows that the material removal rate increases with increases of oxygen pressure at more wt.% of CNT. At higher oxygen pressure and cutting speed that the MRR increases and also observed that lower MRR observed at higher cutting speeds. In case of Al<sub>2</sub>O<sub>3</sub> / CNT the MRR is lower, science alumina is softer in nature (lower hardness) undergoes lower MRR when compared to higher weight of CNT (9%).

## 6. CONCLUSIONS

In the present study, response surface modelling have been carried out using MINITAB software for pulsed Nd: YAG laser straight cutting of Al<sub>2</sub>O<sub>3</sub> / CNT for different wt.% of Carbon nano tubes. Based on the modelling results, following conclusions have been made:

- Al<sub>2</sub>O<sub>3</sub> / CNT for different wt.% of Carbon nano tubes are developed by using so-gel technique.
- The experimental results indicated that low surface roughness (R<sub>a</sub>) and higher material removal rate (MRR) were observed at variation of CNT weight fraction.
- The effect of control parameters on the surface roughness (R<sub>a</sub>) and material removal rate (MRR) has been appraised with the help of taguchi design (L25).
- A quadratic model for surface roughness and material removal rate has been developed from the observed data. The predicted and measured esteems are genuinely near to each other which show that the Ra, MRR and prediction model can be adequately used for predicting the Ra, MRR within the range of process parameters selected in composite materials with 96.27% confidence level
- RSM is found to be more effective for modeling and analysis of surface roughness (R<sub>a</sub>) and material removal rate (MRR) in laser beam machining of developed composites at different combination of design variables such as wt. % of CNT, cutting speed, plus frequency and oxygen pressure.
- Therefore it can be concluded that the higher process parameters, gives better quality results as compared to the results obtained by Taguchi approach only.
- From the response graphs it has been observed that cutting speed has less effect on R<sub>a</sub> as well as MRR compared to other process parameters. For achieving small value of R<sub>a</sub> a higher value of pulse frequency and oxygen pressure is required.

## References

1. A. N. Samant, N. B. Dahotre, Laser machining of structural ceramics – a review, Journal of European Ceramic Society. 29 (2009), pp. 969 – 93.

2. A. N. Samant, Laser machining of advanced material structural ceramics: computational and experimental analysis, PhD dissertation. University of Tennessee, 2009.
3. N. Dahotre, A. Samant, Laser machining of advanced materials, CRC Press, Leiden, 2011.
4. L. Rihakova, H. Chmelickova, Laser Micromachining of Glass, Silicon, and Ceramics, Advances in Materials Science and Engineering, 2015, 6 pp.
5. M. R. H. Knowles et al., Micro-machining of metals, ceramics and polymers using nanosecond lasers. The Int. Journal of Advanced Manufacturing Technology. 1 – 2 (2007), pp. 95 – 102.
6. E. Kacar et al., Characterization of the drilling alumina ceramic using Nd:YAG pulsed laser. Journal of Material Processing Technology. 209 (2009), pp. 2008 – 2014.
7. X. C. Wang, Femtosecond laser drilling of alumina ceramic substrates, Applied Physics A. 101 (2010), pp. 271 – 278.
8. A. S. Kuar, Optimization of Nd:YAG laser parameters for microdrilling of alumina with multiquality characteristics via grey–Taguchi method, Materials and manufacturing processes. 3 (2012), pp. 329 – 336.
9. M. N. Hannon, Experimental and theoretical investigation of the drilling of alumina ceramic using Nd:YAG pulsed laser, Optics & Laser Technology. 4 (2012), pp. 913 – 922.
10. X. C. Wang, High quality femtosecond laser cutting of alumina substrates, Optics and Lasers in Engineering. 6 (2010), pp. 657 – 663.
11. B. S. Zilbas, S. S. Akhtar, C. Karatas, Laser cutting of alumina tiles: Heating and stress analysis, Journal of Manufacturing Processes. 1 (2013), pp. 14 – 24.
12. Y. Yan et al., Experimental and theoretical investigation of fibre laser crack-free cutting of thick-section alumina, Int. Journal of Machine Tools Manufacture. 51 (2011), pp. 859 – 870.
13. H. D. Vora et al., Evolution of surface topography in one-dimensional laser machining of structural alumina, Journal of the European Ceramic Society 32 (2012), pp. 4205 – 4218.
14. H. D. Vora et al., One-dimensional multipulse laser machining of structural alumina: evolution of surface topography, Int. Journal of Advanced Manufacturing Technology, 68 (2013), pp. 69 – 83.
15. H. D. Vora, N. B. Dahotre, Laser machining of structural alumina: influence of moving laser beam on the evolution of surface topography, Int. Journal of Applied Ceramic Technology, (2014), pp. 1 – 14.
16. H. D. Vora, N. B. Dahotre, Surface topography in three-dimensional laser machining of structural alumina, Journal of Manufacturing Processes, 19 (2015), pp. 49 – 58.
17. Poppathi Naresh, S.A. Hussain, B.D. Prasad, A review on multiple responses process parameters optimization of turning Al-TiCp metal matrix composites, Journal of Achievements in Materials and Manufacturing Engineering 80/1 (2017) 32-40.
18. Phadke, M.S. (1989) Quality Engineering Using Robust Design, Prentice-Hall, Englewood Cliffs, NJ.
19. Poppathi Naresh, Syed Altaf Hussain, B. Durga Prasad, “Modeling of Wear Behaviour of AA7068/TiC MMCs Using Fuzzy Logics and Response Surface Model” Materials Focus, vol.7, no. 4, pp.1-9, Dec/2018.
20. Poppathi Naresh, Syed Altaf Hussain, B. Durga Prasad, “Analysis of Dry sliding wear behaviour of AA068/TiC MMCs”, International Journal of Materials Engineering Innovation, vol. 11, no. 1, 2020. DOI:-10.1504/IJMATEI.2020.10026496
21. Montgomery, D.C. (1997) Design and Analysis of Experiments, John Wiley, New York.
22. Cochran, W.G. and Cox, G.M. (1977) Experimental Designs, Asia Publishing House, India.
23. M. Ligo, Influence of laser micromachining parameters on material rate removal and machined surface quality, MTF STU Trnava, 2015.
24. Syed Altaf Hussain, V.Pandurangadu, K.Palani kumar “Cutting power prediction model for turning of GFRP composites using response surface methodology”, International journal of Engineering, Science and Technology, vol.3,No.6, pp-161-171. 2011.

**Biographical notes:**

Yemmani Suresh Babu is a PhD Research Scholar from JNTU Ananthapur under the guidance of Prof. Syed Altaf Hussain and Prof. B. Durga Prasad. He has more than 18 years of experience in teaching and published research publications in repeated journals. His current area of research includes mechanical, wear behaviour and machining behaviour of composites, optimisation techniques and modelling.

Syed Altaf Hussain is a Professor and HOD/Mechanical Engineering, Rajeev Gandhi Memorial College of Engineering and Technology, Nandyal-518501, (A.P), India. He graduated in mechanical engineering from REC Warangal, A.P and post graduated with the specialisation of machine design from JNTUCE Kakinada. He obtained Ph.D degree in faculty of mechanical engineering from JNTUA Ananthapur. He has 25 years of experience in teaching and published a more than 60 research publications in repeated journals. His current area of research includes machining of composite GFRP and AMMCs materials, modern manufacturing, optimisation, simulation and modelling. He is executive council member of ISTE.

Bandaru Durga Prasad is a Professor and Controller of Examination (PG), Department of Mechanical Engineering, JNT University-Anantapur, Anantapuramu-515002, Andhra Pradesh, India. He has more than 25 years of experience in teaching and research and published a more than 100 research publications in repeated journals. His current area of research includes alternative fuels for an I.C Engines, thermal engineering, and machining of composite materials.